Antimicrobial activity and cellular toxicity of nanoparticle–polymyxin B conjugates

2011 Nanotechnology 22 185101

(http://iopscience.iop.org/0957-4484/22/18/185101)

Nanotechnology **22** (2011) 185101 (10pp) doi:10.1088/0957-4484/22/18/185101

Antimicrobial activity and cellular toxicity of nanoparticle–polymyxin B conjugates

Soonhyang Park, Hicham Chibli, Jody Wong and Jay L Nadeau[1]

Department of Biomedical Engineering, McGill University, 3775 University Street, Montreal QC, H3A 2B4, Canada

E-mail: jay.nadeau@mcgill.ca

Received 30 July 2010, in final form 14 February 2011
Published 17 March 2011
Online at stacks.iop.org/Nano/22/185101

Abstract

We investigate the antimicrobial activity and cytotoxicity to mammalian cells of conjugates of the peptide antibiotic polymyxin B (PMB) to Au nanoparticles and CdTe quantum dots. Au nanoparticles fully covered with PMB are identical in antimicrobial activity to the free drug alone, whereas partially-conjugated Au particles show decreased effectiveness in proportion to the concentration of Au. CdTe–PMB conjugates are more toxic to *Escherichia coli* than PMB alone, resulting in a flattening of the steep PMB dose–response curve. The effect is most pronounced at low concentrations of PMB, with a greater effect on the concentration required to reduce growth by half (IC50) than on the concentration needed to inhibit all growth (minimum inhibitory concentration, MIC). The Gram positive organism *Staphylococcus aureus* is resistant to both PMB and CdTe, showing minimal increased sensitivity when the two are conjugated. Measurement of reactive oxygen species (ROS) generation shows a significant reduction in photo-generated hydroxyl and superoxide radicals with CdTe–PMB as compared with bare CdTe. There is a corresponding reduction in toxicity of QD–PMB versus bare CdTe to mammalian cells, with nearly 100% survival in fibroblasts exposed to bactericidal concentrations of QD–PMB. The situation in bacteria is more complex: photoexcitation of the CdTe particles plays a small role in IC50 but has a significant effect on the MIC, suggesting that at least two different mechanisms are responsible for the antimicrobial action seen. These results show that it is possible to create antimicrobial agents using concentrations of CdTe quantum dots that do not harm mammalian cells.

S Online supplementary data available from stacks.iop.org/Nano/22/185101/mmedia

1. Introduction

The emergence of multiply-resistant bacterial strains is rapidly becoming a public health crisis, especially in the case of Gram negative bacteria [5]. A highly promising approach to combat antibiotic resistance is to substitute or complement antibiotic treatment with antimicrobial agents that work by physical disruption of the bacterial cell, a mechanism that genetic resistance often cannot overcome. Nanoparticles may be among the best of these agents, but their toxicity to humans must be measured and the exact mechanisms of their action need to be determined. The concept of nanoparticles as antimicrobials is not new. The antibiotic property of silver (Ag) nanoparticles is well known and they have been used topically and systemically to treat infections by physically destroying bacteria [25]. Bacterial toxicity studies have also been performed with other types of nanoparticles: titanium oxide [7], buckyballs or C60 [31, 20] and carbon nanotubes [20, 6].

Quantum dots (QDs) are fluorescent semiconductor nanoparticles with size-dependent emission spectra that can be excited by a broad choice of wavelengths. The most common types of QDs contain Cd, as this results in spectra that span the visible, examples being CdSe, CdSe/ZnS, and CdTe. All of these types of QDs can act as photosensitizers; they absorb visible light and generate reactive oxygen species (ROS), resulting in cytotoxicity. They can also mediate toxicity through the production of Cd^{2+}, which can induce generation of ROS [19, 29].

Only a few studies have investigated QDs as antimicrobial agents. The evaluation of QD toxicity to bacteria is complex

[1] Author to whom any correspondence should be addressed.

as it is a function of: (1) QD core material and size/color, (2) QD coating, (3) QD conjugation to targeting or antibacterial molecules, (4) bacterial strain, and (5) conditions in which they are used [2, 17]. We have previously reported in detail the antimicrobial activity of unconjugated red/orange CdTe QDs [12, 13]. In those studies, we found that Gram negative strains were much more sensitive than Gram positive strains to CdTe, with IC50 values of ∼50–100 nM when exposed to 30 min of blue light for Gram negatives and values >1 μM for Gram positives. Values were significantly higher when the samples were kept in the dark. Toxicity was related to ROS generation but not to liberation of free Cd^{2+} ions, which were released at very low levels.

In this study, we wished to exploit the sensitivity of Gram negative strains to QDs to create conjugates to antibacterial agents that act in an additive or synergistic fashion, demonstrating antimicrobial activity at very low QD and antibiotic concentrations. Polymyxin B (PMB) is an antibiotic which binds specifically to the lipopolysaccharide portion of Gram negative bacteria [32]. PMB conjugated to silver nanoparticles has shown synergistic effects with PMB [27].

The goal of this study was to quantify the toxicity of various sizes of CdTe QDs to a Gram negative (*Escherichia coli*) and a Gram positive (*Staphylococcus aureus*) bacterial strain, with and without conjugation to PMB. As a comparison, we also prepare PMB conjugates to Au nanoparticles which by themselves are non-toxic to control for effects of nanoparticles alone. We find that PMB–CdTe conjugates are highly effective against *E. coli*, with an additive effect that depends upon light exposure for its action. The conjugates are ineffective against *S. aureus* except at very high concentrations, with a minimal additive effect of CdTe. The effect is due to specific toxicity caused by the CdTe particles, as Au particles of a similar size reduce rather than augment the efficacy of PMB.

For QD conjugates to be potentially useful *in vivo*, they must show minimal toxicity to mammalian cells. In this work we also examine the toxicity of CdTe and CdTe–PMB to NIH3T3 mouse fibroblasts. While CdTe alone shows substantial toxicity, CdTe–PMB is less toxic to these mammalian cells than the QDs alone, with negligible effects at bactericidal concentrations. This suggests that creating highly effective antimicrobial agents with low toxicity to mammalian cells is possible using QDs.

2. Experimental methods

2.1. Au nanoparticle synthesis

The procedure for gold nanoparticle synthesis was adapted from published methods [18]. Hydrogen tetrachloroaurate(III) trihydrate (0.5 mmol) and tiopronin (N-(2-mercaptopropionyl)glycine) (1.2 mmol) were dissolved in 20 ml of methanol/acetic acid 6:1 and an aqueous solution of sodium borohydrate (7.5 ml, 8 mM) was slowly added. After vigorous stirring for 30 min, the resulting black solution was collected and concentrated. The resulting black residues were dissolved in 20 ml of water and dialyzed for 72 h against dH_2O (2 l), which was changed every 12 h.

2.2. CdTe QD synthesis and solubilization

CdTe QDs were synthesized by a procedure using CdO as the precursor [15]. Briefly, 0.026 g (0.20 mmol) of CdO and 0.179 g (0.63 mmol) oleic acid (OA) were added to a three-neck flask containing 10 ml of ODE. This mixture was degassed for 5 min and heated under an N_2 atmosphere to 220 °C until the solution became colorless. In a separate vessel, the tellurium precursor (TOPTe) was prepared by mixing 0.01 g (0.08 mmol) of Te with 0.415 g (1.12 mmol) trioctylphosphine (TOP) and 2 ml ODE under N_2 into a sealed vial. This mixture was vigorously stirred until the solution became light yellow. Next, the temperature of the CdO–ODE mixture was further increased to 310 °C. Formation of a gray Cd^0 precipitate was evident after prolonged heating (10–20 min) of the reaction mixture at 310 °C. Immediately after formation of Cd^0, the TOPTe precursor was rapidly injected. The temperature was allowed to drop and stabilized at 270 °C for the growth of the nanoparticles. Aliquots of the reaction mixture were withdrawn at various time points and injected into cold toluene to quench further growth. QDs were solubilized with mercaptopropionic acid (MPA) using a biphasic approach. 400 μl of toluene, 500 μl of 200 mM phosphate buffered saline (PBS) (pH 9) and 1 μl of MPA were added to 100 μl of concentrated hydrophobic QDs. Following vigorous mixing, the QDs moved from the organic phase to the aqueous phase, which was extracted using a pipette. QDs were isolated from excess thiol by several cycles of concentration and dilution using a filter with a 10 kDa cutoff (Vivaspin).

2.3. Nanoparticle characterization and conjugation

All particles were characterized by ultraviolet–visible (UV–vis) absorbance and fluorescence emission spectroscopy, zeta potential, and transmission electron microscopy (TEM). UV–vis absorbance spectra were recorded on a SpectraMax Plus plate reader (Molecular Devices, Novato, CA) and fluorescence emission spectra on a Gemini EM plate reader (Molecular Devices, Novato, CA). The concentration of Au was determined by lyophilizing and weighing; molar concentration was estimated using a molecular weight calculated from the average particle diameter determined from electron microscopy. CdTe concentrations were calculated from UV–vis absorbance spectra using published methods [33]. Zeta potential was measured using a Zeta plus/Zeta potential analyzer (Brookhaven Instruments Corporation, NY). Samples for TEM were prepared on carbon coated copper grids, and examined with an accelerating voltage of 200 keV on a JEOL JEM-2100F at the Centre de Caractérisation Microscopique des Matériaux, École Polytechnique de Montréal. Also performed were selected area electronic diffraction (SAED) and energy dispersive x-ray spectroscopy (EDS).

Particles were conjugated to PMB by electrostatic assembly as we have published and characterized previously [9]. Briefly, nanoparticles and PMB were mixed at the desired ratio and allowed to self-assemble for 30 min before use. The conjugation efficiency was monitored by UV–vis spectroscopy. Particles were purified of excess PMB by centrifugation and

washing. The amount of PMB bound and the stability of the conjugates were evaluated using the fluorescent ortho-phthaldialdehyde (OPA) assay as previously described [10, 4] in order to quantify unbound PMB in the solution. The OPA solution was prepared by dissolving 1 mg ml^{-1} of OPA in 200 mM borate buffer and 2 μl ml^{-1} beta-mercaptoethanol. For stability analysis, samples kept in the dark were compared with those irradiated with 2.5 mW, 440 nm light. At each time point, samples were withdrawn and unbound PMB was purified from the QD–PMB complex with a 10 K molecular weight cut-off filter (Vivaspin). The filtrate was mixed with OPA solution and incubated for 5 min. OPA was excited at 350 nm and emission was measured at 450 nm and compared with a standard curve to determine the amount of unbound PMB in the solution.

2.4. Measurement of reactive oxygen species (ROS)

The generation of hydroxyl radicals was measured with sodium terephthalate following published methods [3, 26]. Briefly, QDs were mixed with disodium terephthalate (1 mM) (Sigma Aldrich) and irradiated. Aliquots of the reaction mixture were withdrawn at 10 min time intervals, treated with 0.5 volumes of 1 M NaOH and monitored by fluorescence emission with excitation at 300 nm. The colorimetric XTT assay was used to measure $HO_2^{\cdot}/O_2^{-}$ generation [1]. The tetrazolium dye 2,3-Bis(2-methoxy-4-nitro-5-sulfophenyl)-2H-tetrazolium-5-carboxanilide (XTT) (Sigma Aldrich) was added to the QDs at 1 mM. After the indicated period of irradiation, absorbance was measured at 470 nm. The Amplex Red assay was performed using the Amplex red hydrogen peroxide assay kit (Invitrogen) according to the manufacturer's instructions.

2.5. Bacteria

The bacterial strains used were a Gram negative strain (*Escherichia coli* ATCC 10798) and a Gram positive strain (*Staphylococcus aureus* methicillin-resistant clinical isolate). Strains were cultivated aerobically, *E. coli* in Luria Broth (LB; 37 °C, 200 rpm) and *S. aureus* in brain heart infusion (BHI). The IC50 of PMB, QDs, and QD–PMB with and without light exposure were determined from growth curves taken as described previously [13]. Briefly, samples were seeded into 96-well plates and allowed to grow to a determined optical density at 600 nm (OD600), usually 0.1–0.15. The QDs were added and irradiation was performed; the non-irradiated side of the plate was screened with aluminum foil. The plates were then placed into a heated plate reader at 32 °C and read at 600 nm every 10 min for 5–8 h. Growth curves were plotted as OD600 versus time. Curve fits were performed using a Prism 5 for Macintosh OSX (GraphPad software).

2.6. Light exposure

To excite QDs bound to bacteria, irradiation was performed with a custom lamp consisting of 96 2.5 mW, 440 nm LEDs mounted onto a 96-well plate; this lamp is inverted over the sample plate and ensures even application of light.

2.7. Mammalian cell toxicity assays

The toxicity of CdTe and CdTe–PMB were determined using the sulforhodamine B (SRB) assay [21]. The assay was performed using NIH3T3 fibroblast cells grown in Dulbecco's modified eagle medium (DMEM) with 10% fetal bovine serum (FBS) under a 5% CO_2 atmosphere. Cells were passaged at 5×10^3 cells per well in 96-well culture plates 24 h before use. When they had grown to 60% confluency, they were incubated with CdTe alone, PMB alone, or CdTe–PMB at various concentrations for 30 min in serum-free, phenol-red free medium with or without irradiation. The medium was then exchanged for supplemented DMEM and the cells were returned to the incubator. After 24 or 48 h, cells were fixed with trichloroacetic acid (50 μl of 40% v/v) at 4 °C for 2 h, washed five times with distilled water, air-dried overnight and stained with SRB reagent (sulforhodamine) (50 ml) for 30 min. Unbound SRB was removed with acetic acid 1%, bound SRB was dissolved in Tris (100 μl of 10 mM solution at pH 10.5). Absorbance was read at 510 nm. In each plate, at least five or six repeats were done of each condition, and independent assays were performed at least three times.

3. Results

3.1. Nanoparticle and conjugate characterization

The Au nanoparticles were monodisperse, with a mean ± standard error of the mean (SEM) diameter of 2.7 ± 0.7 nm (figures 1(A) and (B)). At this small size, no plasmon peak was evident on the absorbance spectrum. The particles showed a weak far-red fluorescence when excited at 550 nm (quantum yield <1%; emission peak, 780 nm) (figure 1(C)). Three sizes of CdTe nanoparticles, corresponding to three distinct emission colors, were used. They were highly monodisperse, with mean diameters of 3.1 ± 0.2 nm (green-emitting), 3.4 ± 0.3 nm (yellow-emitting), and 4.1±0.7 nm (red-emitting) (figures 1(E) and (F)). For all particles, zeta potential was approximately −40 mV.

Assembly of negatively-charged QDs with polycationic reagents such as PMB occurs spontaneously and rapidly as observed by changes in zeta potential, migration by gel electrophoresis, and aggregation [9, 22]. We found that greater than 40 PMB molecules added per QD-carboxylate led to aggregation and loss of colloidal stability within seconds, and so all further imaging experiments were performed with a 30:1 ratio or smaller of PMB:QD. Such ratios led to complete association of the PMB with the particles, with no free PMB in the supernatant when particles were centrifuged and washed (not shown; free PMB measured by OPA assay). PMB assembly also led to a quenching of 90–95% of the QD emission accompanied by a red-shift of ∼10 nm (figure 2). This was in contrast to what was seen with CdSe/ZnS, which became brighter upon assembly with PMB [9]. The conjugates were stable for at least 5 h with and without 440 nm light irradiation, as evidenced by the lack of PMB released into the solution as measured by the OPA assay (no significant signal at all time points; limit of detection: 100 nM or 1 part in 300; experiment repeated three times).

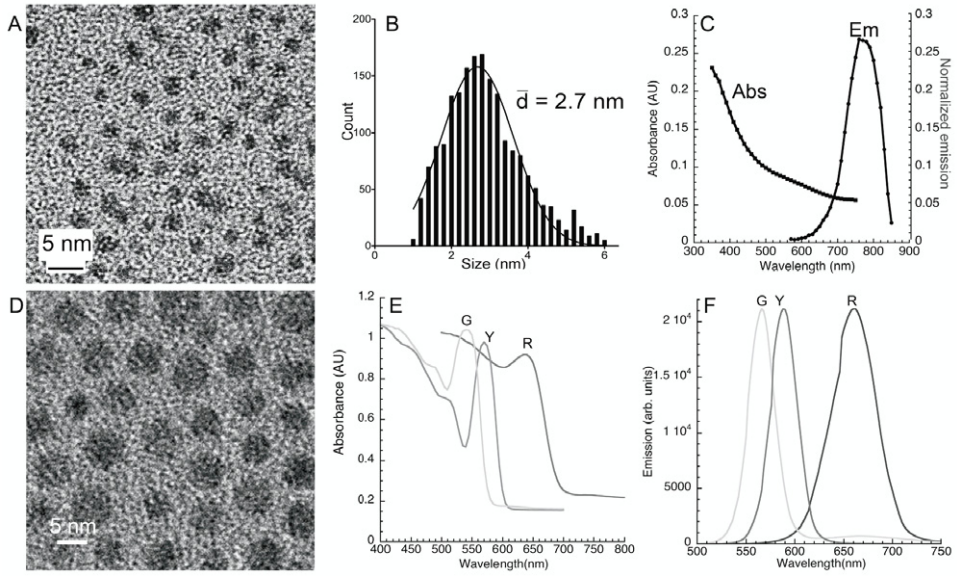

Figure 1. Properties of nanoparticles used in this study: (A) TEM image of Au nanoparticles; (B) size distribution of >1500 particles showing a mean diameter of 2.7 nm; (C) absorbance and emission spectra of Au nanoparticles, because of the small size, there is no plasmon resonance peak; the emission was taken with excitation at 550 nm; (D) TEM image of red CdTe QDs, mean diameter 4.1 nm; (E) absorbance spectra of green (G, mean diameter 3.1 nm), yellow (Y, mean diameter 3.4 nm), and red (R) CdTe QDs; (F) emission spectra of G, Y, and R QDs excited at 400 nm.

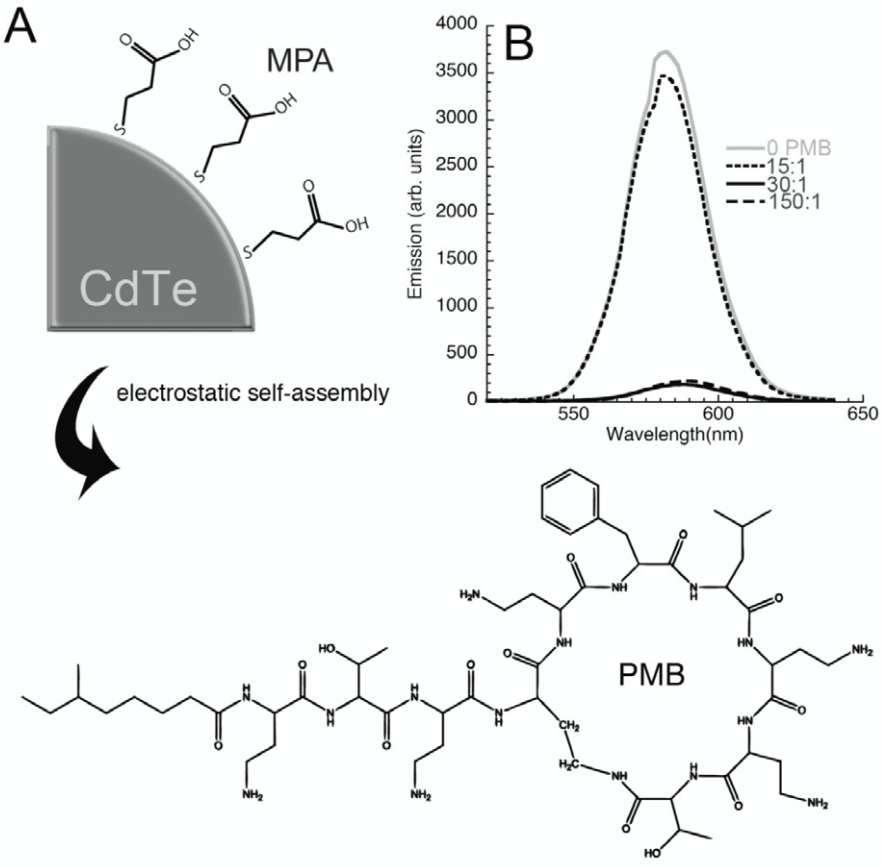

Figure 2. Characterization of QD–PMB. (A) Scheme for the design of QD–PMB; QDs are stabilized by the ligand MPA to provide carboxylate functionality on the surface (above) and the structure of PMB is shown (below). (The tiopronin-capped Au nanoparticles also have carboxylate groups.) (B) Typical emission spectra of CdTe QDs before and after conjugation of PMB at different ratios.

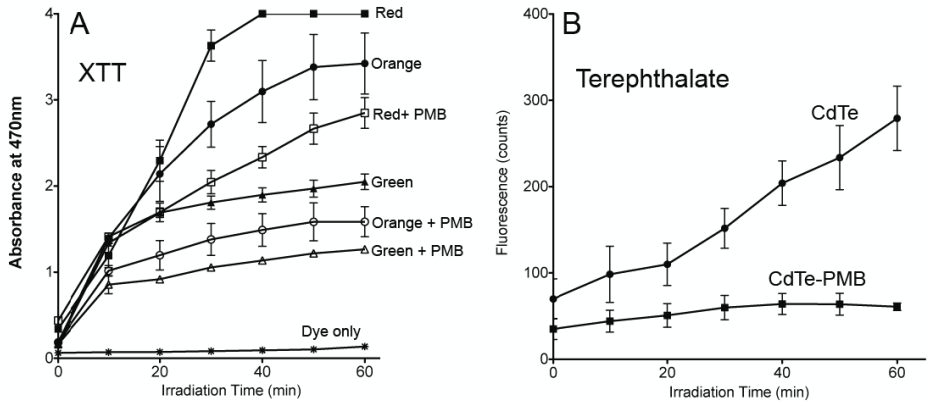

Figure 3. Measurement of ROS generation by CdTe QDs and QD–PMB conjugates. (A) Signal from XTT measured by absorbance at 470 nm versus time of exposure to blue light irradiation. The results are means ± SEM of four independent experiments with duplicates in each. When error bars do not appear, they are smaller than symbols. (B) The sodium terephthalate assay measured as emission at 435 nm with excitation at 300 nm. The results are means ± SEM of four independent experiments with all QD colors averaged (a total of 8–12 data points for each condition).

3.2. Reactive oxygen species (ROS)

We have previously found no sign of singlet oxygen generation from CdTe nanoparticles, but have found evidence of both superoxide and hydroxyl radical production in the presence of water, oxygen, and blue light illumination [13, 12]. We repeated these tests here with CdTe alone and CdTe–PMB conjugates to determine the effect of conjugation on radical formation. The XTT and sodium terephthalate tests have been shown to be consistent in the presence of quantum dots and to agree with spectroscopic measures [11]. XTT measures $HO_2^{\cdot}/O_2^{-}$ generation colorimetrically when the generated radicals reduce the tetrazolium dye 2,3-Bis(2-methoxy-4-nitro-5-sulfophenyl)-2H-tetrazolium-5-carboxanilide (XTT) to the highly colored (yellow) XTT formazan [1]. Sodium terephthalate measures hydroxyl radical formation by the formation of a fluorescent product, 2-hydroxyterephthalate [3, 28]. We also used the Amplex Red assay, which measures H_2O_2 formation by either absorbance or fluorescence emission.

We found a positive XTT signal from all colors of CdTe that varied according to preparation, with the green QDs showing the lowest signal and the red and orange QDs a higher signal. A plateau was seen after 30–50 min of irradiation. All signals were reduced approximately two-fold in the QD–PMB conjugates (figure 3(A)). In contrast, the signal from the sodium terephthalate assay was the same for all QD colors. The signal nearly disappeared upon PMB conjugation (figure 3(B)).

The Amplex Red assay in the presence of CdTe yielded extremely large signals, corresponding to tens of millimolar of H_2O_2 (see supplementary data, figure S1 available at stacks.iop.org/Nano/22/185101/mmedia). It has been previously reported that other types of nanoparticles, including titania and ceria, yield similar erroneous results [16], and so we concluded that Amplex Red was not reliable in the presence of CdTe.

No ROS generation was observed from Au nanoparticles (data not shown).

3.3. Growth curve models, antimicrobial activity of PMB alone and Au–PMB conjugates

Antimicrobial activity of PMB and conjugates was determined from growth curves for *E. coli* and *S. aureus* with PMB and Au–PMB at different concentrations and ratios. This approach provides a dynamic view of toxicity and when properly analyzed yields more information than static measures such as plate counts [23]. All growth curves were fitted to the logistic function

$$y = y_0 + \frac{y_{\max} - y_0}{1 + \exp(\beta - \alpha x)}, \tag{1a}$$

where α corresponds to the growth rate and β to the location parameter (fitting values are provided in supplementary information, table S1 available at stacks.iop.org/Nano/22/185101/mmedia). The exception was for curves where growth was not seen and optical density decreased exponentially; in these cases the curves were fitted to the exponential decay equation

$$y = y_0 + (y_{\max} - y_0)\mathrm{e}^{-kx}. \tag{1b}$$

The bacterial density at a chosen time point was then plotted versus PMB concentration (or in some cases CdTe concentration). This gave an IC50 curve of the form

$$y = y_{\min} + \frac{y_{\max} - y_{\min}}{1 + 10^{[\mathrm{Log(IC50)} - x]H}}, \tag{2}$$

where H is the Hill coefficient. Values of IC50 were compared at 2–3 time points representing mid-log and plateau growth phases and were found to be highly consistent; a mid-log value was then chosen for each of the curves shown here.

Minimum inhibitory concentration (MIC) was also determined from the growth curves by relating the fractional area under the growth curve (AUC) to two parameters, P_1 and P_2 [8]:

$$\frac{\mathrm{AUC}}{\mathrm{AUC}_0} = \exp\left[-\left(\frac{C}{P_1}\right)^{P_2}\right], \tag{3}$$

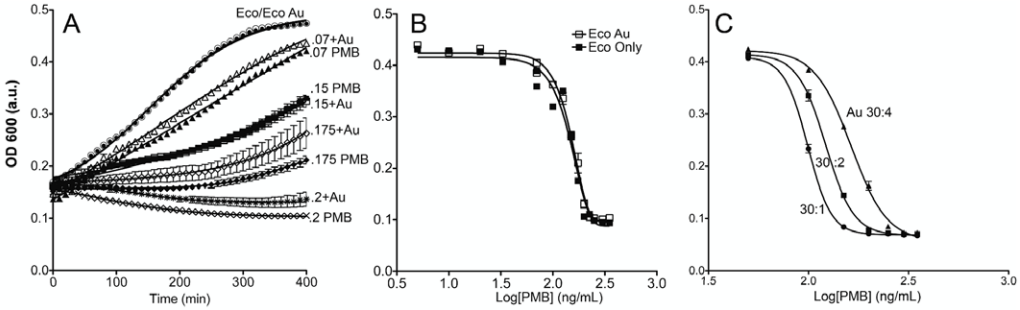

Figure 4. Antimicrobial activity of Au–PMB. (A) Sample growth curves for *E. coli* only (Eco), Au only at 8.5 nM (overlapping), and 0.07, 0.15, 0.175, and 0.2 μg ml^{-1} PMB alone and conjugated 30:1 to Au. Curves are fits to equation (1) with parameters given in the supplementary information, table S1 (available at stacks.iop.org/Nano/22/185101/mmedia). (B) Sample IC50 curves for PMB alone ('Eco only') and with 30:1 PMB conjugates, fitted to equation (2) with fitting values given in the text. There was no significant difference in any experiment between these conditions. (C) IC50 curves for 30:1, 30:2, and 30:4 Au–PMB with fits to equation (2).

where MIC is the intercept of the tangent to the maximum gradient of the curve of AUC versus log $[C]$:

$$\mathrm{MIC} = P_1 \exp\left(\frac{1}{P_2}\right). \tag{4}$$

PMB was highly effective against *E. coli*, with IC50 values of 150 ± 12 ng ml^{-1} and an MIC of 215 ± 20 ng ml^{-1} ($n = 6$ independent experiments). The inhibition curve was very steep with concentration. When PMB was conjugated to Au nanoparticles at a 30:1 ratio, the IC50 was not significantly different from that of PMB alone (145 ± 20 ng ml^{-1}, with some experiments showing a slightly higher value than PMB alone and others slightly lower). The Au particles themselves were non-toxic (figures 4(A) and (B)). Increasing amounts of Au made the conjugates increasingly less effective, with an increase in IC50 of $\sim$20 ng ml^{-1} each time the Au concentration was doubled (figure 4(C)).

As anticipated for Gram positive strains, *S. aureus* was highly resistant to PMB, with IC50 values of 8.5 ± 0.5 μg ml^{-1} and MIC > 15 μg ml^{-1} ($n = 6$ experiments). Conjugation to Au did not make the drug more effective (data not shown).

3.4. Antimicrobial activity of CdTe–PMB

The CdTe QDs used in this study were consistent with those reported previously [12, 13]. For *E. coli*, IC50 values were >200 nM without light exposure and were not fully determined. With 30 min of blue light, values of IC50 were somewhat dependent upon the size of the particles, with smaller particles being more toxic: $\sim$40 nM for green CdTe, $\sim$50 nM for orange, and $\sim$80 nM for red (the difference between green and orange was not statistically significant) (supplementary information, figure S2 available at stacks.iop.org/Nano/22/185101/mmedia). MICs for all colors with light exposure were $\sim$300 nM. *S. aureus* was significantly more resistant to the QDs, with IC50 values >600 nM with or without irradiation (supplementary information, figure S3 available at stacks.iop.org/Nano/22/185101/mmedia).

Because of the high sensitivity of *E. coli* to PMB, bactericidal concentrations of 30:1 PMB: CdTe corresponded to very low concentrations of CdTe. A concentration of 0.05 μg ml^{-1} PMB was the highest tested at which the drug alone showed no significant effect on *E. coli* growth. Conjugated 30:1 to CdTe (corresponding to a CdTe concentration of 1.2 nM), this same concentration caused nearly 50% growth inhibition when exposed to light. At 0.1 μg ml^{-1} PMB and 2.4 nM CdTe, cell growth was almost completely inhibited (figure 5(A)). There were no significant differences in toxicity between the different colors of QDs (data not shown). The overall effect of CdTe conjugation to PMB was a flattening of the very steep PMB dose–response curve, making it nearly linear. While the effects of light were statistically significant at low concentrations, they were very small, and they became negligible at concentrations >100 ng ml^{-1} PMB/2.4 nM CdTe. IC50 values were reduced by nearly a factor of three with CdTe: 57 ± 5 ng ml^{-1} without irradiation, and 55 ± 5 ng ml^{-1} with light (figure 5(B)). The MIC values showed a strong dependence on light; calculated values were 190 ± 20 ng ml^{-1} without irradiation, and 120 ± 20 ng ml^{-1} with 30 min of light exposure (see supplementary information, table S1 for AUC values available at stacks.iop.org/Nano/22/185101/mmedia).

As expected, *S. aureus* showed significant resistance to PMB, with effective concentrations more than ten-fold what was seen for *E. coli*. CdTe was not able to overcome this resistance to any significant degree, even though conjugation to effective drug concentrations corresponded to high concentrations of the nanoparticles. Complete bacterial inhibition could be achieved at 12 μg ml^{-1} PMB/288 nM CdTe (figure 5(C)). Examination of the IC50 curve showed a modest effect of CdTe on growth that was similar across PMB concentrations, and that did not depend upon light exposure. IC50 was reduced to 7 ± 1 μg ml^{-1} (figure 5(D)).

3.5. Synergy or additive effect?

To determine whether PMB and CdTe worked synergistically, the fractional inhibitory concentration (FIC) index was used, where

$$\mathrm{FIC} = \frac{\mathrm{MIC(CdTe[with\ PMB])}}{\mathrm{MIC(CdTe)}} + \frac{\mathrm{MIC(PMB[with\ CdTe])}}{\mathrm{MIC(PMB)}}. \tag{5}$$

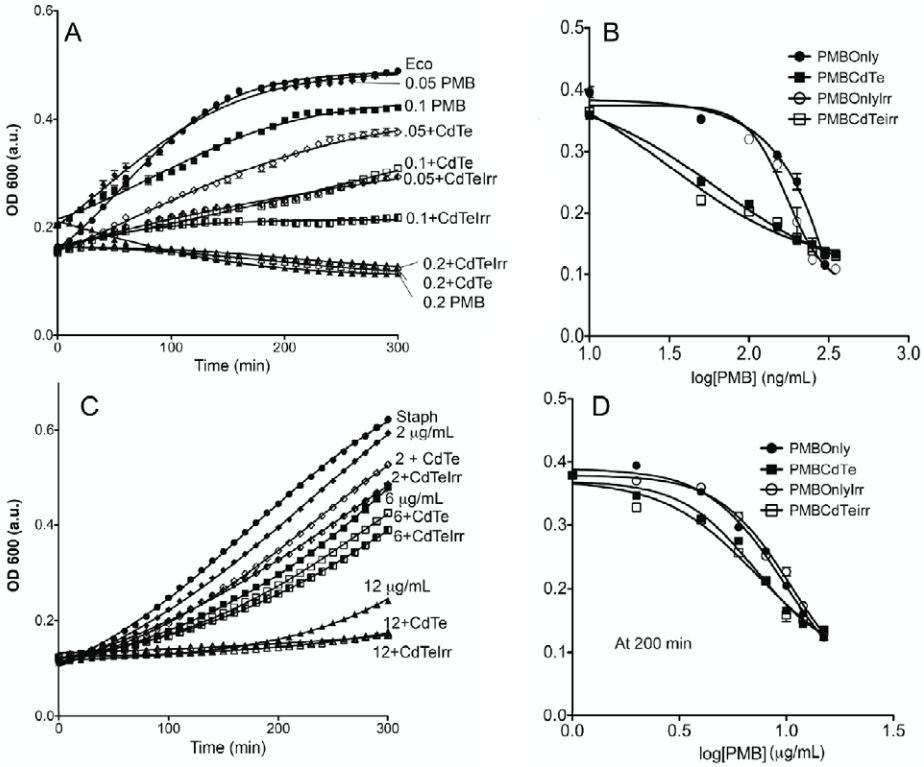

Figure 5. Effects of PMB and PMB–CdTe conjugates on *E. coli* and *S. aureus*. All conjugates are at 30:1 ratios (corresponding to 1.2 nM CdTe: 0.05 μg ml^{-1} PMB). (A) Growth curves of *E. coli* alone (Eco) and with different concentrations of PMB in μg ml^{-1}, those concentrations with CdTe, and the conjugates with 30 min of blue light exposure ('Irr'). Irradiation had no effect on samples not containing CdTe (not shown). Fits are to equation (1) with fit values in the supplementary information, table S1 (available at stacks.iop.org/Nano/22/185101/mmedia). (B) IC50 curves taken at 200 min, fit to equation (2). (C) Growth curves of *S. aureus* alone (Staph) and with different concentrations of PMB in μg ml^{-1}, those concentrations with CdTe, and the conjugates with 30 min of blue light exposure ('Irr'). (D) IC50 curves taken at 200 min, fitted to equation (2).

Table 1. MIC and FIC values for different ratios of PMB:CdTe using green QDs.

Ratio	MIC–PMB (ng ml^{-1})	MIC–PMB (irr)	MIC–CdTe (nM)	MIC–CdTe (irr)	FIC (no irr/irr)
30:1	200	190	4.8	4.6	0.93/0.89
30:2	200	155	9.6	7.4	0.93/0.74
30:4	215	140	21	13.7	1.01/0.70

FIC values <0.5 indicate synergistic activity, whereas values $0.5 < \text{FIC} < 2.0$ indicate additive effects [27]. For 30:1 PMB:QD conjugates, the MIC values corresponded to FIC values of close to unity (table 1). In order to maximize the QD:PMB effects, we examined the results of changing the ratio of PMB to the QDs. It was found that increasing the CdTe concentration for a given PMB concentration led to an increased FIC in the absence of light, but a decrease with light exposure. The lowest FIC value was seen with a 30:4 PMB:CdTe ratio in the presence of light. All values implied an additive effect (table 1).

3.6. Toxicity to mammalian cells

PMB is an antimicrobial agent with low toxicity to mammalian cells. No inhibition of NIH3T3 fibroblasts was seen with PMB concentrations up to tens of μg ml^{-1} (not shown). CdTe showed a concentration-dependent toxicity to these cells that was not dependent upon light exposure, with IC50 values ~60–75 nM for the mean of three colors (figure 6(A)). However, PMB caused a reduction in cytotoxicity to fibroblasts relative to QDs alone. At concentrations that were bactericidal to *E. coli*, the 30:1 PMB:CdTe conjugate caused very little toxicity to fibroblasts, with survival >90%. This represented a significant survival benefit over equivalent concentrations of QDs alone (figure 6(B)).

4. Discussion

Stable conjugates of nanoparticles to antibiotics can lead to greater antimicrobial activity than is seen with either agent alone [24]. Polymyxin B (PMB) disrupts the outer membranes of Gram negative bacteria, thereby potentially exposing the cells to the cytotoxic activity of other agents. A previous study reported highly synergistic effects of Ag nanoparticles and

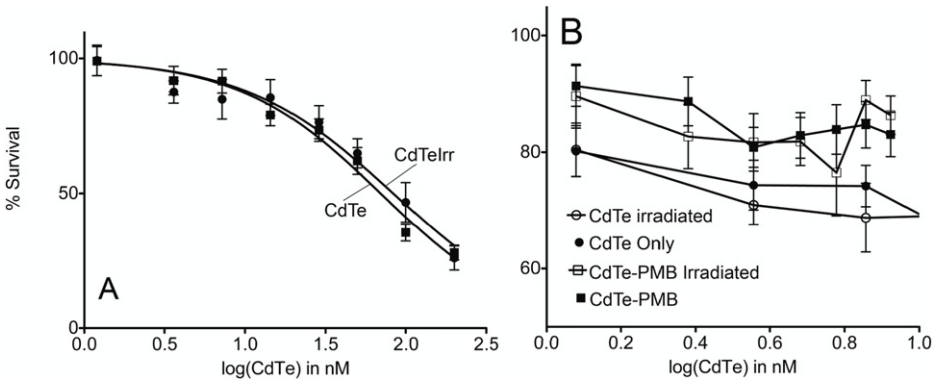

Figure 6. Toxicity of CdTe and CdTe–PMB to mouse fibroblasts. The data are means of three independent experiments with four repeats in each. The independent experiments were each done with a different color of QDs; no significant difference was seen between red, orange, and green so the results were all averaged. (A) CdTe only, with and without irradiation. The lines are fits to equation (1). (B) CdTe–PMB versus CdTe alone at low concentrations. Even at these low concentrations, significant toxicity of CdTe alone is seen. Conjugation to PMB improves cell survival and removes any effect of light exposure. The lines are guides for the eye.

PMB against several Gram negative strains, with FIC values of <0.4 [27].

In this study we examined the antimicrobial activity of Au nanoparticles and CdTe quantum dots conjugated to PMB. One hypothesis to explain increased activity of nanoparticle–antibiotic conjugates is that the conjugate presents a large number of oriented molecules to the cell surface in a small area, thus creating a local concentration that is very high. This mechanism has been invoked to explain the fact that conjugates of Au to vancomycin have shown increased activity relative to the drug alone [14]. If this were the case with PMB, then toxicity of the nanoparticles themselves would not be needed, and even conjugates to non-toxic nanoparticles should show increased activity over PMB alone. This was clearly not the case. Non-toxic Au nanoparticles showed the same activity as free PMB when they were conjugated to the maximum amount of PMB possible without aggregation. When conjugated at smaller ratios, increasing amounts of Au led to proportional decreases in the conjugate's efficacy. We may thus conclude that the conjugation of Au to PMB brings no added benefit as an antimicrobial, and infer that toxicity of the nanoparticles is necessary for an enhanced effect. This is an important negative result, as the generalizability of the vancomycin findings remains largely unknown.

Because we had previously found that Gram negative strains were significantly more sensitive to CdTe than Gram positive strains [13], we expected that the combination of CdTe and PMB would be highly lethal to *E. coli* and much less effective against *S. aureus*. We indeed found increased activity of CdTe–PMB to *E. coli* relative to PMB alone, but with some surprises. The increased activity occurred mostly at the lowest concentrations, leading to a flattening of the dose–response curve. This effect was nearly independent of light exposure. However, effects on the MIC were small. Without light exposure, MIC values of QD–PMB were close to those of PMB alone. Exposure to 30 min of blue light reduced the MICs somewhat, but effects seen were merely additive and not synergistic.

We have previously shown that CdTe QDs release only very low levels of Cd^{2+} ions with 30 min of blue light exposure, and attributed the nanoparticles' antibacterial effects to the photo-generation of reactive oxygen species, particularly hydroxyl and superoxide radicals. There were also secondary effects seen, such as membrane depolarization, which seemed to play a small role in toxicity [12]. In this study we have found that PMB conjugation causes a significant reduction of photo-induced ROS production from CdTe, particularly hydroxyl radicals, which fall nearly to zero. Correspondingly, the toxic effects of CdTe–PMB are less dependent upon light exposure than those of CdTe alone. IC50 values of CdTe with and without light exposure do not show significant differences, suggesting that a significant fraction of *E. coli*—at least half—are sensitive to a non-light-dependent toxicity mechanism of the conjugate. There are several options for what this mechanism might be. The PMB destabilizes the cell membrane, and may therefore allow CdTe to depolarize the cells by affecting the electron transport chain. The small amounts of Cd^{2+} and ROS released even during dark conditions might be highly effective because of their proximity to the cell. The CdTe might also make PMB more reactive by oxidizing the peptide, which could lead to the formation of long-lived ROS species such as peroxide [30]; however, we were not able to adequately address this because of the unreliability of the Amplex Red assay in the presence of quantum dots.

Whatever this mechanism or combination of mechanisms, it is not sufficient to suppress all bacterial growth. Inhibition of all growth requires light exposure and is only a modest improvement over PMB alone. Thus, for at least a significant fraction of the bacteria, phototoxicity of CdTe is necessary for a significant effect, but this effect is small, probably because of the decreased ROS production seen with QD–PMB. We hypothesized that decreasing the PMB coverage on the particles by increasing the ratio of CdTe to PMB would lead to significant reductions in the MIC. This was the case, and the greater the amount of CdTe, the stronger the dependence upon light exposure. However, FIC values remained in the additive range even for the highest ratio tested, which was 30:4.

It is important to note that the CdTe particles in this study were exposed to light only once for a period of 30 min.

Increased time or intensity of light exposure, or exposure at different periods during bacterial growth, may improve the results seen with all of the ratios. It would also be interesting to explore ordinary ambient light or direct sunlight as possible photoactivators of the particles.

The absolute amount of CdTe in the bactericidal conjugates was very small, ranging from 4.8 nM in the 30:1 conjugates to 21 nM in the 30:4 conjugates. This is significantly below the IC50 for fibroblasts, and in fact, PMB conjugation reduces the toxicity of CdTe to NIH3T3 fibroblasts, probably due to the reduction in ROS production. Only the 30:1 ratio was tested, and for further studies this ratio is recommended as increased amounts of Cd do not qualitatively improve antimicrobial activity. This 30:1 ratio is therefore a potentially promising platform for the creation of novel antimicrobial agents for use *in vitro* (e.g. on surfaces) or topically *in vivo*. Further studies are required to exactly determine the mechanisms of action, optimize the light exposure conditions, and determine the toxicity to animals.

Acknowledgments

HC, SP, and JLN acknowledge the US EPA—Science to Achieve Results (STAR) program grant no R831712, the National Science and Engineering Research Council of Canada (NSERC) Individual Discovery program, and the NSERC/Canadian Institutes of Health Research (CIHR) Collaborative Health Research Program (CHRP). JW acknowledges the NSERC CREATE Program (Canadian Astrobiology Training Program).

References

[1] Able A J, Guest D I and Sutherland M W 1998 Use of a new tetrazolium-based assay to study the production of superoxide radicals by tobacco cell cultures challenged with avirulent zoospores of Phytophthora parasitica var nicotianae *Plant Physiol.* **117** 491–9

[2] Aruguete D M, Guest J S, Yu W W, Love N H and Hochella M F 2010 Interaction of CdSe/CdS core–shell quantum dots and pseudomonas aeruginosa *Environ. Chem.* **7** 28–35

[3] Barreto J C, Smith G S, Strobel N H P, McQuillin P A and Miller T A 1994 Terephthalic acid (THA): a dosimeter for the detection of hydroxyl radicals *in vitro Life Sci.* **56** PL89–96

[4] Benson J R and Hare P E 1975 O-phthalaldehyde: fluorogenic detection of primary amines in the picomole range. Comparison with fluorescamine and ninhydrin *Proc. Natl Acad. Sci. USA* **72** 619–22

[5] Boucher H W, Talbot G H, Bradley J S, Edwards J E, Gilbert D, Rice L B, Scheld M, Spellberg B and Bartlett J 2009 Bad bugs, no drugs: no ESKAPE! An update from the Infectious Diseases Society of America *Clin. Infect. Dis.* **48** 1–12

[6] Chatterjee D K, Fong L S and Zhang Y 2008 Nanoparticles in photodynamic therapy: an emerging paradigm *Adv. Drug Deliv. Rev.* **60** 1627–37

[7] Chen F, Yang X, Xu F, Wu Q and Zhang Y 2009 Correlation of photocatalytic bactericidal effect and organic matter degradation of TiO_2. Part I: observation of phenomena *Environ. Sci. Technol.* **43** 1180–4

[8] Chorianopoulos N G, Lambert R J, Skandamis P N, Evergetis E T, Haroutounian S A and Nychas G J 2006 A newly developed assay to study the minimum inhibitory concentration of Satureja spinosa essential oil *J. Appl. Microbiol.* **100** 778–86

[9] Clarke S, Mielke R E, Neal A, Holden P and Nadeau J L 2010 Bacterial and mineral elements in an arctic biofilm: a correlative study using fluorescence and electron microscopy *Microsc. Microanal.* **16** 153–65

[10] Clarke S J, Hollmann C A, Aldaye F A and Nadeau J L 2008 Effect of ligand density on the spectral, physical, and biological characteristics of CdSe/ZnS quantum dots *Bioconjug. Chem.* **19** 562–8

[11] Cooper D R, Dimitrijevic N M and Nadeau J L 2010 Photosensitization of CdSe/ZnS QDs and reliability of assays for reactive oxygen species production *Nanoscale* **2** 114–21

[12] Dumas E, Gao C, Suffern D, Bradforth S E, Dimitrijevic N M and Nadeau J L 2010 Interfacial charge transfer between CdTe quantum dots and gram negative versus gram positive bacteria *Environ. Sci. Technol.* **44** 1464–70

[13] Dumas E M, Ozenne V, Mielke R E and Nadeau J L 2009 Toxicity of CdTe quantum dots in bacterial strains *IEEE Trans. Nanobiosci.* **8** 58–64

[14] Gu H, Ho P L, Tong E, Wang L and Xu B 2003 Presenting vancomycin on nanoparticles to enhance antimicrobial activities *Nano Lett.* **3** 1261–3

[15] Kloper V, Osovsky R, Kolny-Olesiak J, Sashchiuk A and Lifshitz E 2007 The growth of colloidal cadmium telluride nanocrystal quantum dots in the presence of Cd-0 nanoparticles *J. Phys. Chem.* C **111** 10336–41

[16] Lee C W, Chen Y C and Ostafin A 2009 The accuracy of amplex red assay for hydrogen peroxide in the presence of nanoparticles *J. Biomed. Nanotechnol.* **5** 477–85

[17] Wang L, Zheng H, Long Y, Gao M, Hao J, Du J, Mao X and Zhou D 2010 Rapid determination of the toxicity of quantum dots with luminous bacteria *J. Hazardous Mater.* **177** 1134–7

[18] Lopez-Cartes C, Rojas T C, Litran R, Martinez-Martinez D, de la Fuente J M, Penades S and Fernandez A 2005 Gold nanoparticles with different capping systems: an electronic and structural XAS analysis *J. Phys. Chem.* B **109** 8761–6

[19] Lu Z, Li C M, Bao H, Qiao Y, Toh Y and Yang X 2008 Mechanism of antimicrobial activity of CdTe quantum dots *Langmuir* **24** 5445–52

[20] Markovic Z and Trajkovic V 2008 Biomedical potential of the reactive oxygen species generation and quenching by fullerenes (C60) *Biomaterials* **29** 3561–73

[21] Martin A and Clynes M 1993 Comparison of five microplate colorimetric assays for *in vitro* cytotoxicity testing and cell-proliferation assays *Cytotechnology* **11** 49–58

[22] Mattoussi H, Mauro J M, Goldman E R, Anderson G P, Sundar V C, Mikulec F V and Bawendi M G 2000 Self-assembly of CdSe–ZnS quantum dot bioconjugates using an engineered recombinant protein *J. Am. Chem. Soc.* **122** 12142–50

[23] Mueller M, de la Pena A and Derendorf H 2004 Issues in pharmacokinetics and pharmacodynamics of anti-infective agents: kill curves versus MIC *Antimicrob. Agents Chemother.* **48** 369–77

[24] Pissuwan D, Cortie C H, Valenzuela S M and Cortie M B 2010 Functionalised gold nanoparticles for controlling pathogenic bacteria *Trends Biotechnol.* **28** 207–13

[25] Rai M, Yadav A and Gade A 2009 Silver nanoparticles as a new generation of antimicrobials *Biotechnol. Adv.* **27** 76–83

[26] Rajendran V, Lehnig M and Niemeyer C M 2009 Photocatalytic activity of colloidal CdS nanoparticles with different capping ligands *J. Mater. Chem.* **19** 6348–53

[27] Ruden S, Hilpert K, Berditsch M, Wadhwani P and Ulrich A S 2009 Synergistic interaction between silver nanoparticles and membrane–permeabilizing antimicrobial peptides *Antimicrob. Agents Chemother.* **53** 3538–40

[28] Saran M and Summer K H 1999 Assaying for hydroxyl radicals: Hydroxylated terephthalate is a superior fluorescence marker than hydroxylated benzoate *Free Radic. Res.* **31** 429–36

[29] Schneider R, Wolpert C, Guilloteau H, Balan L, Lambert J and Merlin C 2009 The exposure of bacteria to CdTe-core quantum dots: the importance of surface chemistry on cytotoxicity *Nanotechnology* **20** 225101

[30] Stadtman E R 1993 Oxidation of free amino acids and amino acid residues in proteins by radiolysis and by metal-catalyzed reactions *Annu. Rev. Biochem.* **62** 797–821

[31] Tegos G P, Demidova T N, Arcila-Lopez D, Lee H, Wharton T, Gali H and Hamblin M R 2005 Cationic fullerenes are effective and selective antimicrobial photosensitizers *Chem. Biol.* **12** 1127–35

[32] Tsubery H, Ofek I, Cohen S and Fridkin M 2000 The functional association of polymyxin B with bacterial lipopolysaccharide is stereospecific: studies on polymyxin B nonapeptide *Biochemistry* **39** 11837–44

[33] Yu W W, Qu L H, Guo W Z and Peng X G 2003 Experimental determination of the extinction coefficient of CdTe, CdSe, and CdS nanocrystals *Chem. Mater.* **15** 2854–60